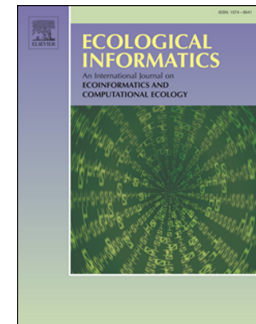# Journal Pre-proof

Lake surface water temperature in China from 2001 to 2021 based on GEE and HANTS

Song Song, Jinxin Yang, Linjie Liu, Gale Bai, Jie Zhou, Deirdre McKay

Please cite this article as: S. Song, J. Yang, L. Liu, et al., Lake surface water temperature in China from 2001 to 2021 based on GEE and HANTS, *Ecological Informatics* (2024), https://doi.org/10.1016/j.ecoinf.2024.102903

Lake surface water temperature in China from 2001 – 2021 based on GEE and HANTS

Song Song[1], Jinxin Yang[1,*], Linjie Liu[1], Gale Bai[1], Jie Zhou[2], Deirdre McKay[3]

[1]*School of Geography and Remote Sensing, Guangzhou University, 510006, Guangzhou, China*

[2]*Key Laboratory for Geographical Process Analysis & Simulation of Hubei Province, College of Urban and Environmental Sciences, Central China Normal University, 430079, Wuhan*

[3]*School of Life Sciences, Keele University, Newcastle-under-Lyme, ST5 5BG, UK*

[*] Corresponding author, yangjx11@gzhu.edu.cn

Abstract: Warming of lakes' surface water leads to accelerated loss of biodiversity and eco-environmental collapse of aquatic systems. Changes in lack surface water temperature (LSWT) are a crucial indicator of lake warming. LSWT growth potentially leads to a higher greenhouse gas emissions and deterioration of the ecological environment within lake systems. However, the magnitude of these changes remains uncertain due to data limitations, particularly for small lakes (1-5 km^2). Small lakes will experience increasing perturbation with accelerating climate change and our methods demonstrate how the impacts of changes in lakes can be accurately measured and monitored. Our study assessed the spatial and temporal patterns of LSWT in China from 2001 to 2021. We utilized Google Earth Engine (GEE) and the Harmonic Analysis of Time Series (HANTS) algorithm to reconstruct LSWT series and detect spatiotemporal dynamics. The innovative connection of GEE and HANTS provides powerful tool for LSWT analysis. Our results show LSWT increased at a rate of 0.24°C per decade, albeit with notable spatial and temporal variations. The nighttime rate of increase was greater than the daytime rate of increase. However, there was an abrupt change in daytime LSWT in approximately 2010 and this occurred earlier than an abrupt change in nighttime LSWT. Geographically, the lakes in the Eastern Plain zone exhibited the most significant LSWT warming trend. The majority of lakes warmed more rapidly between 2011 and 2021 as compared to 2001 to 2010. We found a concurrent and pronounced increase in the frequency of algal bloom occurrences after 2010. Our results demonstrate how GEE and HANTS can deliver the continued monitoring and assessment of LSWT trends needed to inform management strategies aimed at mitigating potential negative impacts of climate change on lake ecosystems, both locally and globally. Building on this method, future research should explore the underlying mechanisms driving LSWT trends and their long-term impacts on lake health.

Keywords: Spatiotemporal variation, Lake surface water temperature, China, GEE, HANTS, climate change

1. Background and summary

Lakes provide naturally circulating water resources crucial for supporting ecological environments, human societies, and economic systems (Oki and Kanae, 2006; Wang et al., 2024). Lake surface variables - e.g. surface water temperature, eutrophication, and carbon emissions – show significant responses to global warming (Jia et al., 2024; Meng et al., 2024; Woolway et al., 2020). Warming trends of lake surfaces have matched or even surpassed the average rate of air temperature change (Butcher et al., 2015; Jia et al., 2022; Woolway et al., 2020). Small lakes, defined as those with an area between 1 and 5 km², are more sensitive to climate warming. Because small lakes have relatively shallow depths and smaller water volumes, they exhibit lower self-regulatory capacities compared to larger lakes. Small lakes thus serve as rapid indicators of warming trends and sentinels of environmental change. In small lakes, even minor fluctuations in lake temperature can have significant impacts on crucial physical and biological processes through nonlinear dynamics (Adrian et al., 2009; Cai et al., 2023). Small lakes numerically dominate the total number of lakes globally, despite contributing minimally to the total lake surface area (Pi et al., 2022; Song et al., 2022; Verpoorter et al., 2014). They contribute disproportionately to local inland water variability and carbon emissions growth (Holgerson and Raymond, 2016; Pi et al., 2022). While excluding small lakes from regional water analysis misrepresents the global aquatic eco-environment (Hanson et al., 2007), it is challenging to include small lakes without adequate data on changes in temperature.

Lake surface water temperature (LSWT) is closely linked to water body temperature. LSWT exhibits greater sensitivity due to the direct exchange of energy between the water surface and the atmosphere (Fairall et al., 1996; Noori et al., 2023). The diverse range of lake sizes and shapes implies that global patterns of LWST are likely to exhibit considerable spatial and temporal variability. Accurately evaluating the warming of LSWT is crucial for assessing the thermal response of all lakes to global change and for developing targeted and effective mitigation strategies to safeguard the ecological integrity of lakes worldwide (Ho et al., 2019; Li et al., 2022). Because previous estimates of LSWT were constrained by technology, these estimates primarily focused on larger water bodies. Small lakes were often omitted.

Omission of small lakes shaped a 2015 global synthesis of *in situ* and satellite-derived LWST data that reported an average increase of 0.34°C decade⁻¹ in summer (O'Reilly et al., 2015a). However, the global mean obscures effects on smaller scales, such as landscape and local scales, where physiography and geomorphology have a more significant influence on the thermal processes of water bodies (O'Sullivan et al., 2019). In China, this same omission has shaped numerous evaluations of LSWT that have concentrated on large lakes in the Tibetan Plateau and Yungui Plateau regions (Wan et al., 2017). As a result of technical limitations, vast lake areas with strong anthropogenic thermal interference have yet to be assessed. Fortunately, recent advances in remote sensing enable long-term synchronous observation and ensure timeliness, effectively addressing this issue.

Remote sensing can support LSWT data extraction across various spatiotemporal scales. LSWT data derived from MODIS (Moderate-resolution Imaging Spectroradiometer) imagery has demonstrated high reliability and is recommended for analyzing long-term spatiotemporal dynamic changes in

LSWT (Sharaf et al., 2019; Tavares et al., 2020; Wan et al., 2017). However, the promotion and utilization of MODIS-based LSWT produce two challenges. First, extracting and processing such extensive datasets is time-consuming and labor-intensive. Second, partial data gaps or imagery of suboptimal quality due to cloud or precipitation can introduce significant bias (Xu et al., 2013). MODIS cloud-contaminated pixels often result in data gaps or produce extreme low temperatures (Xu et al., 2013). Wu et al (2002) estimate over 67% of pixels are lost per year in MODIS LSWT products (Wu et al., 2022). Thus, MODIS imagery alone can lead to substantial bias in estimating lake surface temperature trends.

To compensate, using Google Earth Engine (GEE) to extract LSWT has proven advantageous (Gorelick et al., 2017). GEE can process large-scale datasets, ensure automation and efficiency in data analysis, access diverse data sources, and provide robust visualization and interactivity features (Gorelick et al., 2017; Tamiminia et al., 2020). Fourier-based Harmonic Analysis of Time Series (HANTS) algorithm has also proven to be efficient to mitigate the influence of cloud cover and to preserve the periodic signals of LSWT (Menenti et al., 1993; Verhoef et al., 1996; Zhou et al., 2015). Combining the two should enable more precise monitoring and analysis of LSWT in small lakes.

This study reconstructed 1 km gridded LSWT using the GEE-HANTS algorithm to assess LSWT in lakes larger than 1 km² in China from 2000 - 2021. It assessed the effectiveness of the combined algorithm in detecting patterns and trends in LSWT. The results reveal spatial and temporal changes in LSWT across various lake systems in China. These findings enrich the global LSWT dataset, encompassing a broad spatial coverage and accommodating geomorphic variability across a spectrum of lake sizes. Doing so, they improve understanding of LSWT in China and provide a theoretical foundation for advancing conservation and sustainable utilization of lake ecosystems, particularly those of small lakes, thus can potentially shape lake management and conservation efforts globally.

2. Data and Methods

2.1 Study area

China, spans an extensive area of 9.6 million km², encompassing a diverse array of climates and landscapes. China's vast geographical expanse – between 18-54°N and 73-135°E - holds a wide spectrum of lake ecosystems, ranging from freshwater to alpine lakes. These lakes have been categorized into six distinct zones based on both physical and anthropogenic characteristic. These are: the Qinghai-Tibet Plateau (QT), Inner Mongolia (IM), Xinjiang (XJ), Northeastern Plain (NE), Eastern Plain (EP), and Yunnan-Guizhou Plateau zones (YG) (Figure 1).

Across China, there are a total of 3,741 lakes which each exceed an area of 1 km² (National Tibetan Plateau Data Center). The QT lake zone accounts for approximately one-third of the total lake count and contributes approximately half of national lake surface area. However, the distribution and abundance of these lakes are susceptible to climate variation and anthropogenic activities. Recent years have seen an increase in the overall lake surface area across China (Song et al., 2022). This trend exhibits significant spatial heterogeneity. Alpine lakes in the QT and XJ lake zones have increased significantly in surface area. Changes in cumulative surface area underscore the dynamic nature of lake ecosystems and their interconnections with broader environment changes and anthropogenic activities (Feng et al., 2023; Song et al., 2022).
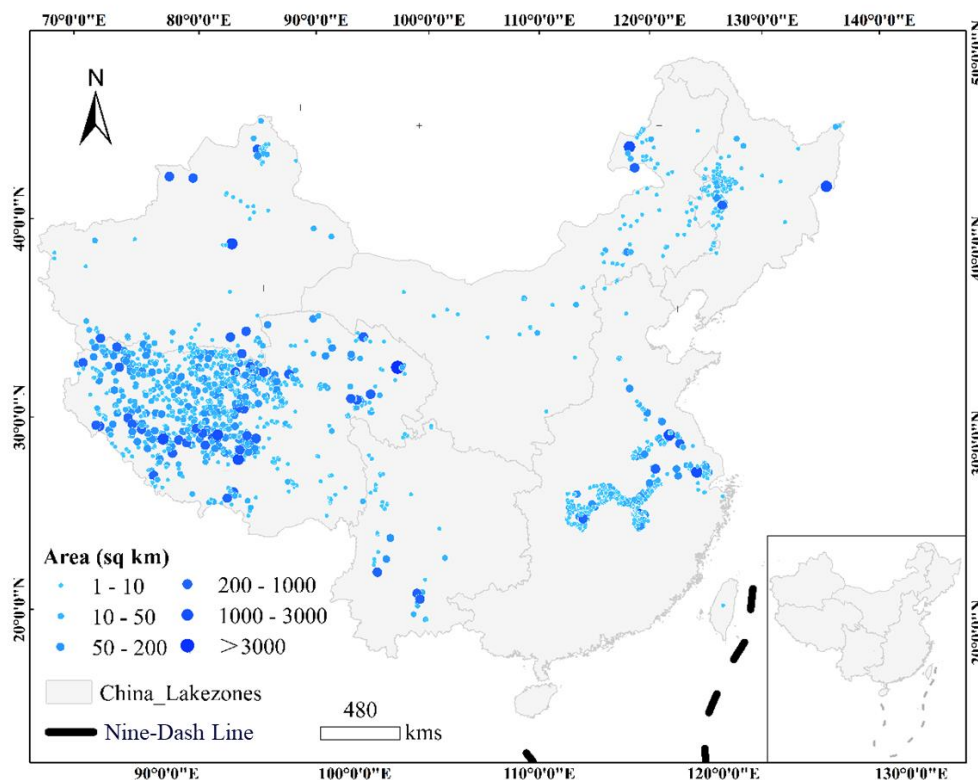
Fig. 1. The distribution of lakes across China's six lake zones

2.2 Data sources

Thermal infrared imagery from satellite remote sensing provides a cost-effective method for monitoring LSWT on extensive spatial and temporal scales (Piccolroaz et al., 2020a; Sharaf et al., 2019). Regular field observations are both scare and costly, while previous studies have demonstrated the reliability of MODIS-derived LSWT data compared to other remotely sensed data (Tavares et al., 2019; Zhang et al., 2014). MODIS datasets, accessible via the Terra (a.m.) and Aqua (p.m.) satellites, consist of 36 spectral bands and produce daily Land Surface Temperature (LST) products known as MOD11A1 and MYD11A1 (Table 1). MOD11A1 is sampled at approximately 10:30 a.m. and 10:30 p.m., while MYD11A1 is collected at approximately 1:30 p.m. and 1:30 a.m. These products are derived using the general split-window algorithm, and the validation accuracy is better than 1 K in most conditions (Wan, 2008). Our derived dataset covers a time period from 2001 to 2021. However, not all pixels are available daily due to cloud coverage.

2.2.1   Data mining

To eliminate the interference of lake expansion or shrinkage, only lakes with stable extents from 2001 to 2021 were selected. This sample encompassed a total of 1,451 lakes, with an area greater than or equal to 1 km², of which approximately half were small lakes (726 lakes with an area >1 and <5 km²). The average LSWT for each lake was then computed based on the lake's pixel values using the Google Earth Engine (GEE). GEE provides a robust solution for lake temperature abstraction by leveraging cloud-based computing capabilities (Gorelick et al. 2017). Unlike traditional tools like

ENVI, which require local image downloads and sequential processing, GEE operates within the Google Cloud, enabling rapid and large-scale batch processing without spatial or temporal limitations. Data on distribution and occurrence of lakes were obtained at five-year intervals from the China lake dataset (1960s-2020) from the National Tibetan Plateau Data Center (http://data.tpdc.ac.cn) (Zhang et al., 2019). Additionally, data on algal blooms (Hou et al., 2022) were collected as an indicator of the ecological impact .

2.2.2   Validation

To validate the accuracy of the MODIS data, *in situ* measurements of LSWT from selected lakes the TP zone (Zhu, 2021) were collected. This field observation dataset comprises daily *in situ* lake water temperature measurements for 124 closed lakes from 2009 to 2020. The observational data in this dataset cover a total lake area of 24,570 km² (53% of the total lake area of the TP). Hourly and daily LSWT data published by Shi and Wang were also collected (Shi and Wang, 2023, 2022). The hourly data are based on the integration of remote sensing observations and the FLake model, which is driven by ERA5-Land during simulation (https://doi.org/10.11888/Terre.tpdc.300662). Daily LSWT was simulated using a hybrid model, Air2Water, coupled with satellite data (https://doi.org/10.11888/Terre.tpdc.300801). Both datasets have undergone rigorous validation using satellite observations and *in situ* measurements, resulting in average correlation coefficients of 0.97 for the hourly data and 0.96 for the daily data. Table 1 shows the full set of data sources this study combined.

Table 1 Data sources

Data	Data source	websites
MODIS-LST（MOD+MYD）	NASA LP DAAC at the USGS EROS Center	https://lpdaac.usgs.gov/products/mod11a2v061/ https://lpdaac.usgs.gov/products/myd11a2v061/
Lake boundary polygon data	National Tibetan Plateau Data Center	http://poles.tpdc.ac.cn/zh-hans/data/fa8426c0-d3f0-4615-8e78-0465a0957891/
In situ measurement data of lake temperature	National Tibetan Plateau Data Center	http://poles.tpdc.ac.cn/zh-hans/data/341740b5-8eac-4dbf-9af1-5d3649ce5629/?q=in-situ
Published hourly and daily LSWT	Dataset of lake surface water temperature in China (1950-2100)	https://cstr.cn/18406.11.Terre.tpdc.300662
	Daily scale dataset of lake surface water temperature and lake surface water	https://cstr.cn/18406.11.Terre.tpdc.300801

	temperature after removing heat extremes in China (1985-2022)	
DEM	NASA / USGS / JPL-Caltech	https://cmr.earthdata.nasa.gov/search/concepts/C1546314043-LPDAAC_ECS.html
Land cover data	NASA LP DAAC at the USGS EROS Center	https://lpdaac.usgs.gov/products/mcd12q1v061/

2.3 Reconstruction of LSWT

The Harmonic Analysis of Time Series (HANTS) model integrates smoothing and filtering techniques to analyze time series derived from remote sensing imagery. The HANTS algorithm represents functions or signals as a superposition of periodic harmonic components through the application of the least squares method. By utilizing iterative least squares fitting, HANTS removes outliers influenced by clouds. Procedures for optimizing the HANTS configuration are reported by Menenti et al., 2016; Xie and Fan, 2021; Zhou et al., 2021). The core formula for data reconstruction within the HANTS framework is provided as follows (Xie and Fan, 2021):

$$Y'(t_j) = a_0 + \sum_{i=1}^{nf}[a_i \cos(2\pi f_i t_j) + b_i \sin(2\pi f_i t_j)] \qquad (1)$$

$$Y(t_j) = \tilde{Y}(t_j) + \xi(t_j) \qquad (2)$$

where Y', Y, and ξ represent the original values, the smoothed series, and the error series, respectively. t_j, where j ranges from 1 to n, denotes the observation time of T, with n representing the maximum number of observations within a given time series. nf corresponds to the number of periodic terms present in the time series, indicating the quantity of harmonic components associated with specific frequencies. The coefficients of the trigonometric components associated with these frequencies are designated as f_i, a_i, and b_i.

Three key parameters control the iteration procedure for HANTS. These are: the fitting error tolerance (FET), degree of over-determination (DoD), and "Hi/Lo" flag . (Menenti et al., 1993; Zhou et al., 2021, 2015) provide comprehensive detail on HANTS iteration. In this study, HANTS was implemented on GEE to provide scalable reconstruction services for multiple remote sensing products (Zhou et al., 2023), i.e. the LWST data. Our team fitted the time series of LSWT on an annual basis using harmonic components of annual, 6-month, and 4-month periods to account for intra-annual variations, combined with a 24-month component to capture short-term inter-annual variations (nf = 4). For this, the FET was set to 5°C, DoD to 5 samples, and "Hi/Lo" flag to "Low,". By addressing the limitations created by cloud cover, HANTS-reconstructed MODIS image products offer more precise reflection of temperature change trends, enhancing data fidelity. Figure 2 shows HANTS fitting of MODIS data for two lakes in the EP and QT zone, a) Gaibacuo Lake (2 km^2) and

b) Xiangjiadang Lake (1.06 km^2). HANTS-reconstructed data can mitigate uncertainty and capture the trend of variations in long-sequence LSWT.
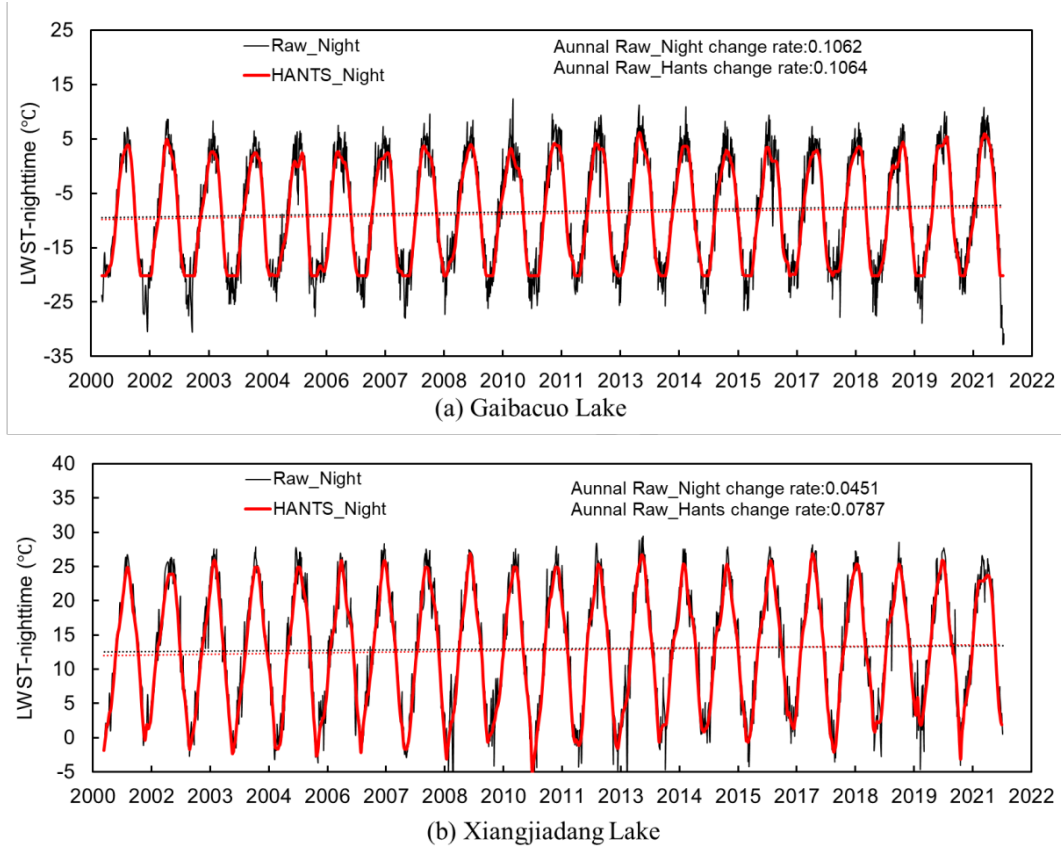

Fig. 2. HANTS fitting based on MODIS data for two small lakes in the EP and QT zone

2.4 Trend and abrupt change analysis

Annual mean LSWT were calculated based on the 8d-averaged LSWT data. The temporal variation trends of the LSWT were then estimated based on a linear regression analysis (Wan et al., 2017; Zhang et al., 2014).

$$Y=AX+B+E \qquad (3)$$

here Y denotes the LSWT, X is the corresponding year, A represents the changing rate of the temperature, B means the intercept, while E indicates the residuals of the prediction (differences between the actual and estimated values of Y). The abrupt change of LSWT was carried out based on Man-Kendall test.
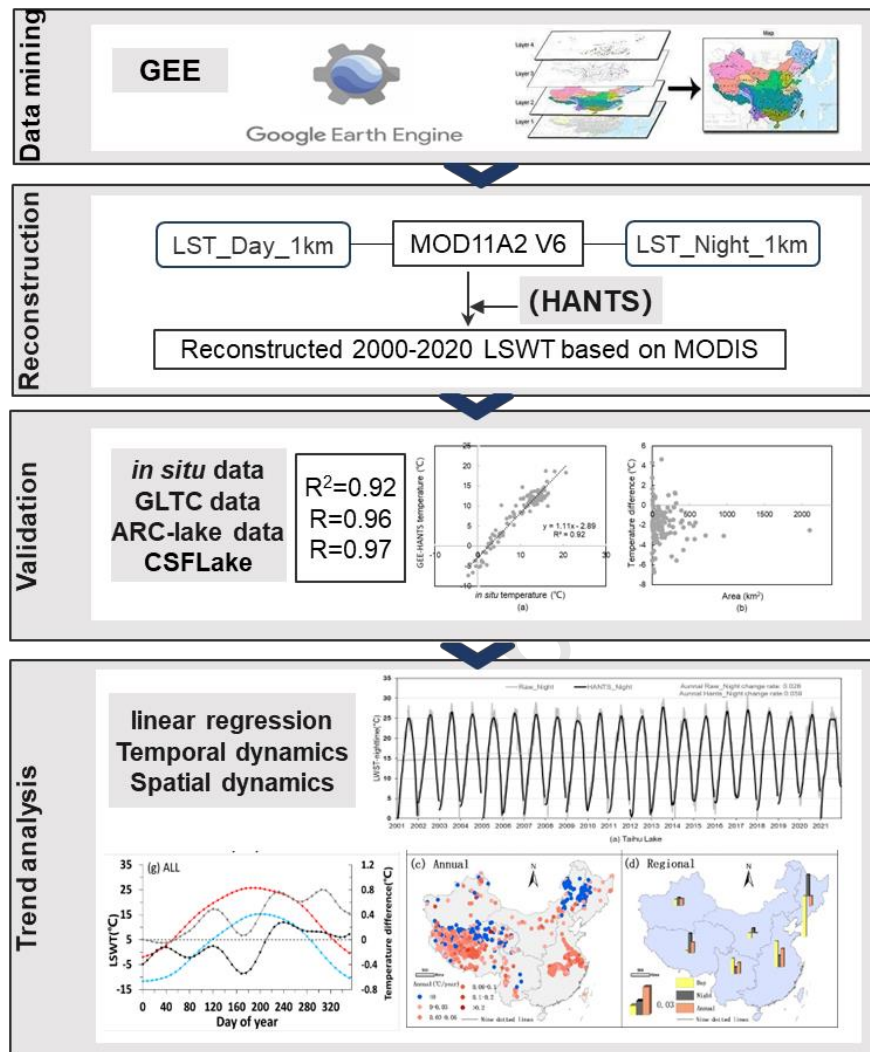
Fig. 3. The flow chart of this study

3. **Results**

3.1 Validation of LSWT reconstructed by HANTS

The MODIS LSWT dataset demonstrates a significant level of agreement with global databases. It coincides with GLTC (R=0.97) and ARC-Lake data (R=0.96), thereby confirming their credibility in capturing extensive temperature patterns (Wan et al., 2017). The reliability of the *in situ* LSWT measurements for 124 closed lakes in TP zone, established by sensors and validated in previous studies (Wu et al., 2024; Zhu, 2021), provides a robust basis for validation. LSWT data reconstructed by HANTS including 118 of the 124 lakes, aligns closely with the *in situ* data, exhibiting a high coefficient of determination (R^2=0.92) (Figure 4a). The data show that, as lake size increases, the temperature differences tend to decrease (Figure 4b). LSWT reconstructed by HANTS is comparable to *in situ* measurements from the TP zone, with the LSWT being approximately 1.81°C lower than *in situ* (Zhu, 2021). For small lakes - smaller than 5 km² but greater than 1 km² - the absolute error of LSWT reconstructed by HANTS was approximately 2.48°C (Table 2). Therefore, the HANTS

algorithm used in this study is valid in capturing LSWT dynamics. Our results show the HANTS algorithm can both be applied across vast regions and include small lakes (1-5 km²).
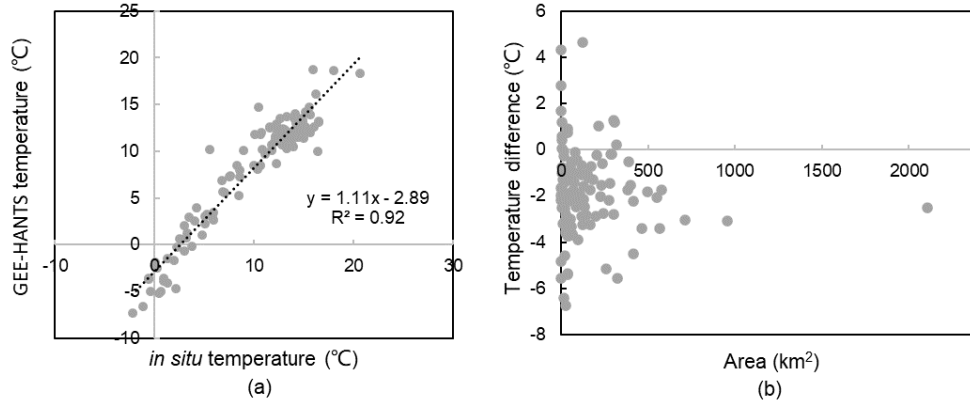

Fig. 4 Temperature comparison between MODIS and *in situ* measurement in 118 selected lakes in TP (Tibetan Plateau): (a) fitting line of MODIS and *in situ* measurement; (b) temperature difference of different lake area

Table 2 Temperature difference for LSWT in 12 small lakes (<1,<5 km²) in Tibetan Plateau zone

Lake_Name	Date of measurement	longitude	latitude	Area (km²)	Temperature difference (°C)
Bandong Lake_1	2016/11/3	89.362	33.163	3.05	-2.50
Bangong Lake_2	2017/8/30	79.809	33.551	1.55	2.79
Deru Co_1	2016/11/9	88.912	32.671	1.66	-2.00
Freshwater Lake_1	2012/10/22	88.752	33.436	2.23	-4.82
Gyaring Co_1	2017/7/2	88.485	31.015	2.32	4.31
Liangxi Lake	2012/10/28	88.466	34.606	1.40	-5.58
Ma'erxia Co_1	2018/9/6	87.553	30.954	1.63	-1.67
Nam Co_1	2016/6/25	90.776	30.768	1.04	1.68
Wuma Co_1	2018/9/17	83.177	32.438	3.33	0.40
Yamdrok Lake_1	2019/7/23	90.867	28.948	3.81	-1.01
Yueya Lake_1	2012/10/27	88.385	34.383	1.79	-2.17
Zhari Namco_1	2009/9/17	85.717	30.902	3.65	-0.78
Average				2.29	-0.95

Linear regression analysis conducted between our HANTS data and the published hourly and daily products reveals a high degree of consistency among the datasets. For the hourly data, we selected 92,445 LSWT samples according to satellite transit times, and the fitting results are presented in formula (3). For the daily results, 406,261 samples with temperatures exceeding 1°C were chosen, and the corresponding results are shown in formula (4). These analyses further underscore the reliability and accuracy of our approach in estimating LSWT.

$$Y = 0.94x_1 + 0.57 \qquad R^2=0.95 \qquad (3)$$
$$Y = 0.91x_2 + 0.87 \qquad R^2=0.93 \qquad (4)$$

Here, Y represents the HANTS data, x_1 and x_2 are the selected hourly and daily LSWT.

3.2 LSWT trend

3.2.1 LSWT temporal trend

The temporal trends of LSWT are shown in Figure 5. Generally, LWST increase during nighttime (0.17-0.47 °C decade^{-1}) was greater that of daytime (-0.15-0.42 °C decade^{-1}). The exceptions were in the EP and YG zones, where the daytime LWST was rising is slightly faster than nighttime. Daytime LWST tended to decline in NE and IM lake zones. According to the annual overall data for LWST, EP represented the greatest increasing trend with 0.42 °C decade^{-1}, while the NEP zone had the lowest rate of increase in LSWT, with only 0.17 °C decade^{-1}.
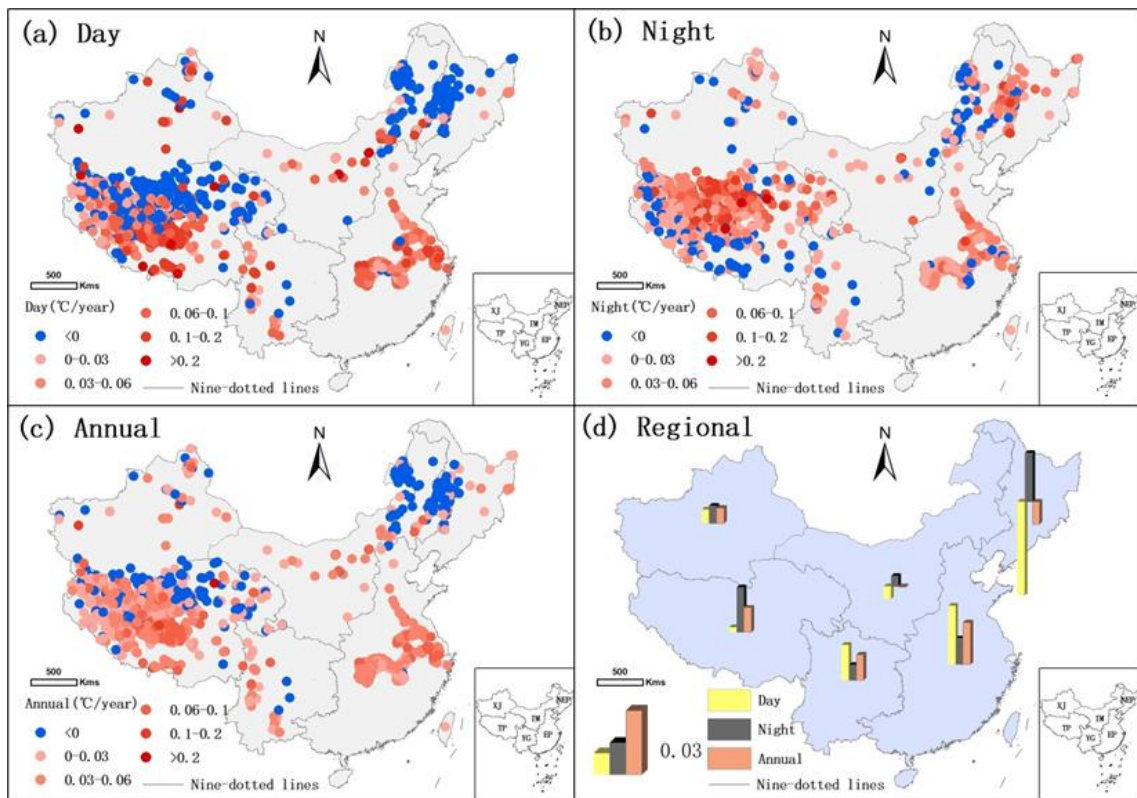

Fig. 5. Temporal trends in LSWT

3.2.2 LSWT spatial dynamics

Trends for LSWT in China's six lake zones are shown in Table 3. The warming trend dominated the majority of lakes, except daytime and overall LSWT in the NE zone. Only 4 out of 99 lakes in the NE zone showed significant warming during the day, while the rest 95 lakes tend to cool during daytime ($p<0.1$). Although nearly all the lakes were warming during nighttime, only 34 out of 140 lakes were on an overall warming trend. In the IM zone, one third of lakes show a cooling trend, with 47.5% of lakes colling during the day and 37.5% cooling during the night. In northwestern China (TP and XJ), 40%-46% lakes presented a cooling trend during daytime, while only 2.6%-12% lakes were cooling during nighttime. Nighttime temperatures revealed a more distinct increasing trend in both overall rate and percentage of warming, compared to daytime temperatures.

Table 3 LSWT trends for all 1,451 lakes in the six lake zones

Lake zones	Time	Warming			Cooling			p<0.1		
		No.	Percentage	rate (°C/y)	No.	Percentage	rate (°C/y)	No.	Warming	Cooling
EP (444)	Day	429	96.60%	0.063	15	3.40%	-0.019	318	100%	0.00%
	Night	406	91.40%	0.030	38	8.60%	-0.008	187	98.90%	1.10%
	Overall	441	99.30%	0.044	3	0.70%	-0.003	367	100%	0.00%
IM (95)	Day	38	40%	0.084	57	60%	-0.078	40	52.50%	47.50%
	Night	58	61.10%	0.033	37	38.90%	-0.024	24	62.50%	37.50%
	Overall	42	44.20%	0.037	53	55.80%	-0.031	30	66.70%	33.30%
NEP (140)	Day	13	9.30%	0.026	127	90.70%	-0.109	99	4%	95.00%
	Night	132	94.30%	0.053	8	5.70%	-0.008	92	100%	0.00%
	Overall	34	24.30%	0.017	106	75.70%	-0.036	58	15.50%	84.50%
TP (663)	Day	380	57.30%	0.059	283	42.70%	-0.069	233	53.20%	46.80%
	Night	576	86.90%	0.055	87	13.10%	-0.02	382	97.40%	2.60%
	Overall	550	83.00%	0.035	113	17%	-0.022	217	92.60%	7.40%
XJ (75)	Day	41	54.70%	0.082	34	5.30%	-0.067	40	60.00%	40.00%
	Night	58	77.30%	0.035	17	22.70%	-0.039	25	88.00%	12.00%
	Overall	53	70.70%	0.033	22	29.30%	-0.023	30	86.70%	13.30%
YG (34)	Day	27	79.40%	0.057	7	20.60%	-0.044	19	84.20%	15.80%
	Night	26	76.50%	0.025	8	23.50%	-0.014	8	100.00%	0.00%
	Overall	29	85.30%	0.034	5	14.70%	-0.02	19	94.70%	5.30%

Note: No. refers to the number of the lakes with warming or cooling trend. The number in the parentheses refers to the number of lakes of the corresponding lake zone.

3.3 Abrupt change in LSWT

3.3.1 Detection of abrupt change in LSWT

Detecting abrupt change of LSWT provides a more precise understanding of the dynamic process of temperature change and reveals underlying driving mechanisms (Ratajczak et al., 2018). We applied the Mann-Kendall (M-K) test to detect the abrupt change point of lakes in the six lake zones. Our results indicate that most abrupt change points occurred between 2005 and 2010 (Figure 6). Overall, daytime LSWT exhibited a faster response to general climate warming and anthropogenic interference, and abrupt changed earlier than nighttime LSWT, except in the NEP zone.
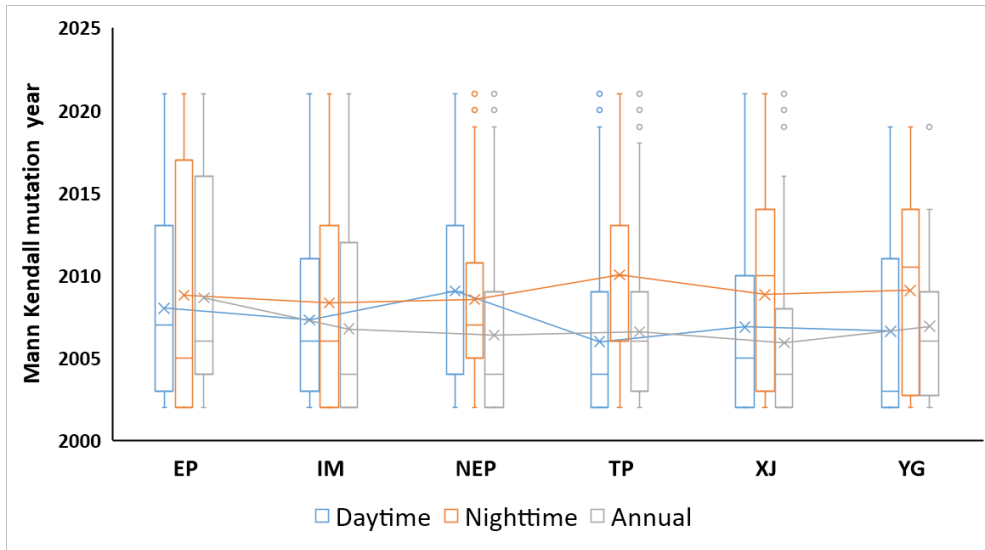
Fig. 6. Abrupt change points for daytime and nighttime LSWT in each of China's six lake zones

3.3.2 LSWT change over time

The average LSWTs during daytime (red) and nighttime (blue) for the entire study period (2001-2021) are shown in Figure 7. Informed by our M-K test results, we took 2010 as the average point. This average abrupt change point enabled us to divide the overall study time period into an earlier (2001-2010) and a later time period (2011-2021). The average daytime (black) and nighttime (grey) LSWT of the earlier and later periods were calculated, and the LSWT differences from the earlier period to later period (LSWT difference=$LSWT_{later}$-$LSWT_{earlier}$) are shown in Figure 6. Changes in LSWT exhibit strong spatial differences. Generally, nighttime warming surpassed daytime warming (Fig.6 g), except in the EP and YG zone. LSWT in most zones displayed the highest range of increase during spring, seen in lakes in EP, MP, NEP and XJ zones. However, a cooling trend occurred in the TP zone in the same season. This difference might be attributable to increased meltwater from glaciers and the snowcap in the TP zone. LSWT in YG zone is exceptional, with the smallest difference in increase difference between daytime and nighttime LWST, and a similar range of increase across the four seasons. Overall, the pattern of LSWT increase for China follows the trend for the TP zone because more than one third of the small lakes studied are found in this zone.
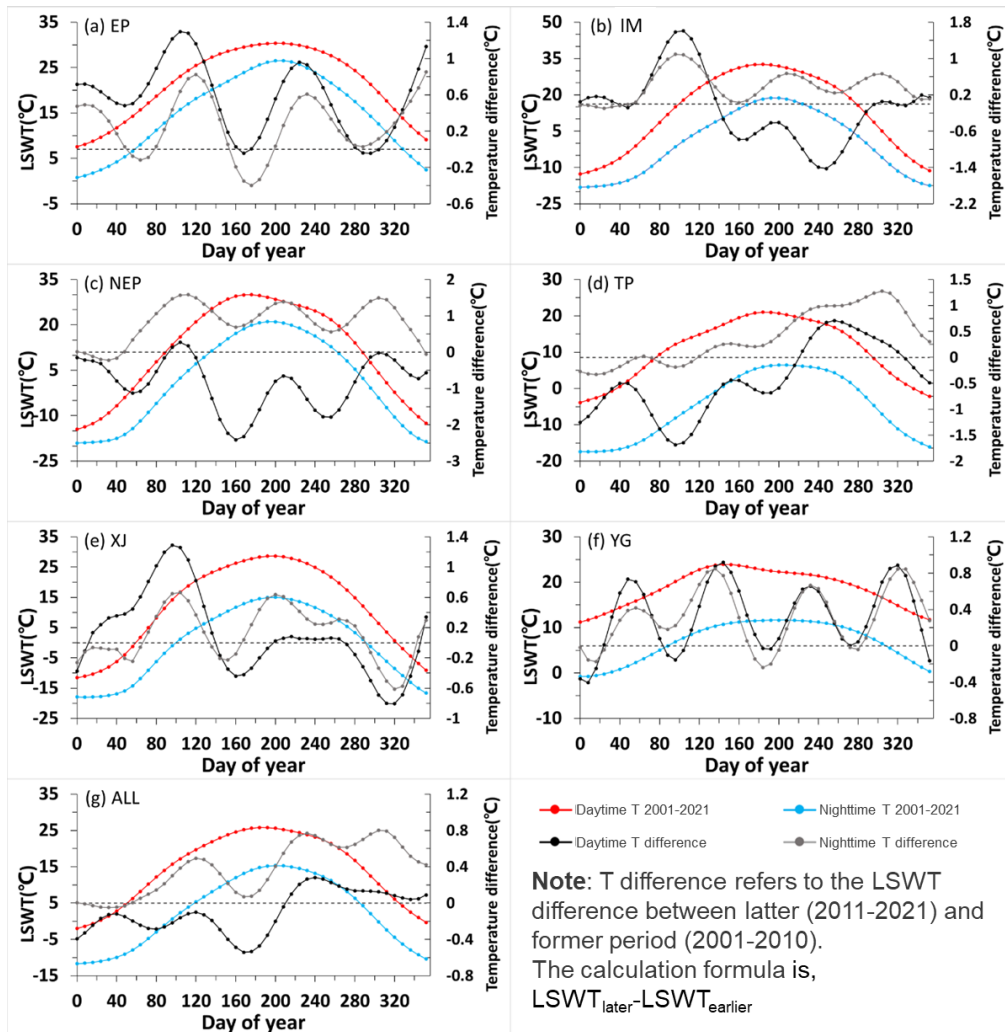
Fig. 7. Annual LSWT of all lakes in each of China's six lake zones

3.4 LSWT and lake characteristics

The LSWT warming trend for each lake is influenced by lake characteristics. Typically, larger lakes exhibit greater stability in LSWT and thus a smaller warming trend (Fig. 8a). Our results demonstrate that lakes with areas ranging from 1 to 5 km² display a warming rate that spans from -0.68 to 1.13 ℃ per decade, whereas lakes exceeding 100 km² exhibit a narrower warming range of -0.29 to 0.61 ℃ per decade.

The relationship between elevation and LSWT is more complex. China's lakes are primarily found in the lowlands and on high plateaus. Lakes situated in low-elevation areas (<100m) demonstrate the highest and most stable warming trends. Conversely, for elevations exceeding 100m, the warming rate of LSWT positively correlates with elevation (Fig. 8b). This complex interaction between lake characteristics and environmental conditions underscores the need for a nuanced understanding of LSWT warming trends to determine their potential impacts on lake ecosystems.
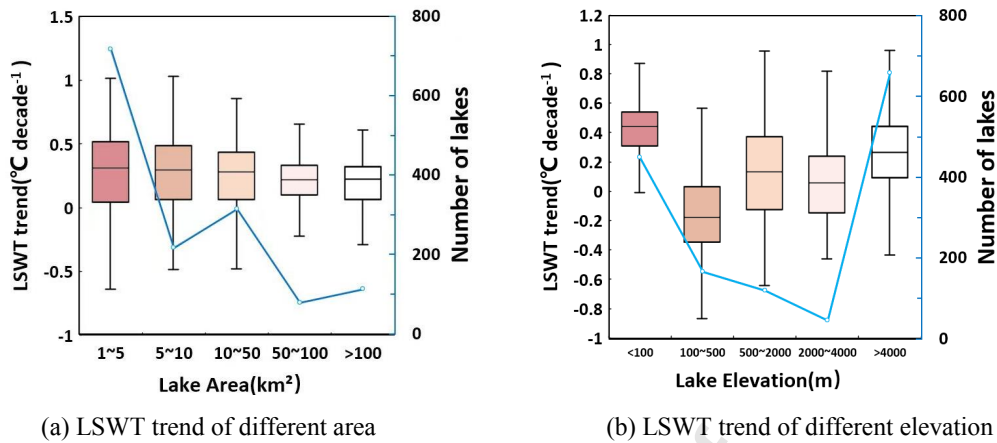
(a) LSWT trend of different area   (b) LSWT trend of different elevation

Fig. 8. LSWT warming trend for lake groups by a) area and b) elevation

4. Discussion

4.1 China's LSWT warming trend

Our method enabled our research to encompass a broader spectrum of lakes, representing the most extensive, comprehensive, and diverse LSWT data set to date for China. By surpassing previous studies, e.g. Xie et al.'s (Xie et al., 2022) study of 126 lakes (area > 50 km^2), and Huang et al.'s (Huang et al., 2023, 2021) examination of approximately 90 large lakes (area > 100 km^2).

We found LSWT of small lakes warmed more rapidly than that of big lakes. Compared with that of big lakes, LSWT for small lakes was more sensitive to environmental change, showing stronger increasing (0.41 vs 0.34 °C/decade) or decreasing (-0.34 vs -0.22 °C/decade) trends during the study period, except in EP and XJ lake zones (Fig. 9). In EP, both small and big lakes showed similar warming trends. One big lake and two small lakes were on a non-significant cooling trend. while the bigger lakes showed a higher cooling trend. In XJ lake zone, most small lakes showed a significant warming or a non-significant cooling trend. The four lakes with a significant cooling trend were located near snow-capped mountains and are big lakes fed by snow meltwater.
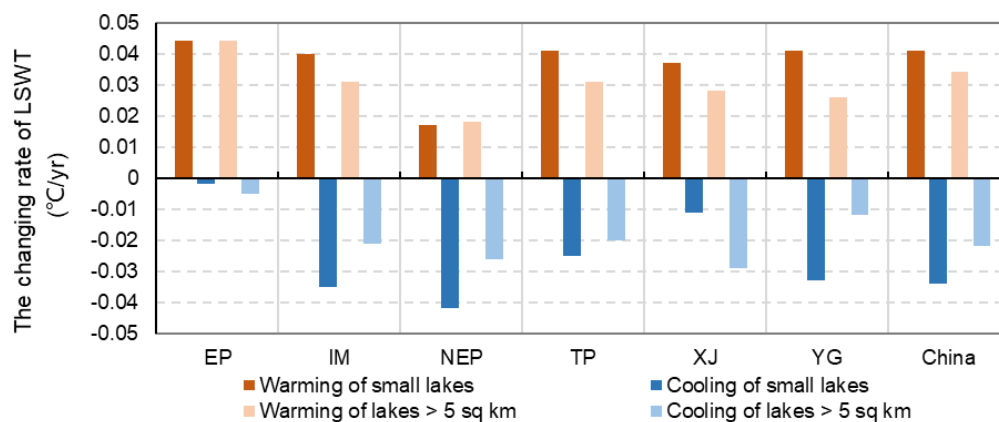

Fig. 9. Change rates in LSWT for small lakes (1-5 km^2) and lakes larger than 5 km^2

4.2 Comparison to wider patterns

The warming trend observed in our analysis over the past two decades tends to be lower compared with national and global pattern (Table 4). This discrepancy may be attributed to the exclusion of temperatures below 0 °C. These negative temperature values represent ice surface temperatures during winter and early spring, when LSWT increases more rapidly (Guo et al., 2022; Virdis et al., 2020). Another explanation may be that our study period also encompasses the global warming hiatus (circa 2000-2012) (Winslow et al., 2018). During this period, LSWT growth was subdued, due to its strong dependence on air warming. Another reason for the discrepancy may be that modelled LSWT warming trends tend to exceed those derived from satellite and *in situ* measurements. For example, Flake's model tends to overestimate the LSWT warming trend across China (Wang et al., 2023). This discrepancy between modelled and in situ data underscores the necessity of further model validation to mitigate the uncertainties associated with warming and cooling trends (Jia et al., 2022; Piccolroaz et al., 2024). LSWT changes exhibit considerable variation, influenced by factors such as the number, size, and location of selected lakes, as well as the study period and methodology adopted. Therefore, more regional studies of the dynamic response of LSWT to environmental change which integrate multiple data sources are needed (Jia et al., 2022; Virdis et al., 2024).

In our study, lakes in the EP zone demonstrate the most pronounced warming rate. This is consistent with previous studies (Huang et al., 2023; Liu et al., 2015; Piccolroaz et al., 2020). While LSWT in the TP zone has garnered extensive research attention, studies here have yielded varied results. This variation can be attributed to discrepancies in research time series, methodologies adopted for addressing freezing period, and distinct temperature sampling techniques.

Table 4 Comparing our results to results of previous research

Regions	Research period	Data source	Temperature	Trend (°C/decade)	Trend of our research (°C/decade)	
					All	≥50km²
Global	1981-2020 (Tong et al., 2023)	Flake model calibrated with Landsat	Overall	0.24	0.24	0.19
	2001-2020 (Tong et al., 2023)			0.25		
	1973-2014 (Piccolroaz et al., 2020)	air2water	Winter	0.35		
			Summer	0.32		
	1985-2009 (O'Reilly et al., 2015a)	*in situ* and satellite	Overall	0.34		
China	2000-2016 (Xie et al., 2022)	MODIS	Day	0.21	0.12	0.08
			Night	0.31	0.36	0.31
			Overall	0.26	0.24	0.19
			Warming lakes	0.38	0.62	0.38
			Cooling lakes	-0.21	-0.78	-0.37
	1979-2018 (Huang et al., 2023)	Flake	Overall	0.4	0.24	0.19
			Warming lakes	0.53	0.62	0.38
			Cooling lakes	-0.64	-0.78	-0.37
TP	1978-2017 (Guo et al., 2022)	Modis air2water	overall	0.01-0.47	0.24	0.19
	2001-2012	Modis	overall	0.12±0.33	0.24	0.19

	(Zhang et al., 2014)		Warming lakes	0.55±0.33	0.35	0.23
			Cooling lakes	-0.53±0.38	-0.22	-0.17
	2001-2015 (Wan et al., 2018)	Modis	Overall	0.37	0.25	0.17
			Warming lakes	0.76	0.35	0.23
			Cooling lakes	-0.53	-0.22	-0.17
	2000-2015 (Song et al., 2016)	Modis	Warming lakes (day)	0.4	0.59	0.34
			Warming lakes (night)	0.51	0.55	0.35
			Cooling lakes (day)	-0.6	-0.69	-0.37
			Cooling lakes (night)	-0.62	-0.2	-0.15
YG	2001-2017 (Yang et al., 2019)	Modis	day	0.91	0.36	0.28
			night	0.58	0.16	0.27
	1979-2018 (Huang et al., 2023)	Flake	overall	0.12	0.26	0.27
EP		Flake	overall	0.49	0.43	0.42
Taihu	2002-2013 (summer) (Liu et al., 2015)			0.59±0.53	0.47	
Dianchi	1980-2017 (Peng et al., 2021)			0.36	0.28	
Qinghai Lake	2001-2010 (Huang et al., 2017)			0.1	0.18	

Against the general trend of increasing LSWT, some lakes exhibit distinct cooling trends. These lakes are predominantly located in the northwestern TP, northern IM, and the NEP zones, primarily fed by glacier and permafrost meltwater. In the northwestern TP zone, permafrost degradation has been documented as the primary driver behind the expansion of lake volumes and observed lake surface cooling (Jiang et al., 2017; Wan et al., 2018). In our study, around 7%, 33%, and 84% of the lakes studied in TP, IM, and NEP, respectively, showed an annual cooling trend ($p<0.1$). The prevalence of cooling during daytime was significantly higher compared to nighttime, with 46% TP, 47% IM, and 95% NEP of lakes experiencing daytime cooling versus 2% TP, 33% IM, and 0% NEP during the night ($p<0.1$). This is in accordance with prior studies, which have highlighted contrasting trends in long-term LSWT, with cooling during daylight hours and warming during the night (Wan et al., 2017). The disparity between day and night likely stems from faster melting of ice and snow during the day, which can introduce more cold water into the lakes, subsequently leading to a decrease in LSWT. Conversely, during night, when temperatures drop and melting is reduced, the impact of melt water on LSWT diminishes.

4.3 Ecological impacts of lake warming

Lake warming tends to intensify eutrophication, increasing carbon emissions, especially in small and shallow lakes (Hu et al., 2024; Kumar et al., 2023; Rao et al., 2024). Increasing LSWT is one of the best predictors for the occurrence of algal blooms (Descy et al., 2016). Polynomial regression modeling with historical data and pigment records reveals that warming explains 78% of observed cyanobacterial biomass trends (Bartosiewicz et al., 2019a). Large lakes are vulnerable to eutrophication because warmer LSWT results in an earlier onset, higher intensity and longer duration of stratification, while simultaneously decreasing dissolved oxygen (Woelmer et al., 2024; Woolway

and Merchant, 2019; Yaghouti et al., 2023). Whether lakes are large or small, increasing LSWT means that taking action to reduce external nutrient inputs alone may not effectively mitigate eutrophication (Filiz et al., 2020; Lürling and Mucci, 2020; Meerhoff et al., 2022).

Small lakes contribute disproportionately higher emissions of greenhouse gases as compared to larger lakes (Holgerson and Raymond, 2016; Pi et al., 2022). High nutrient loading in small lakes may intensify the effect of LSWT warming by stimulating carbon production (Kumar et al., 2023; Xiao et al., 2022). This involves complex dynamics. The impact of thermal shielding and eutrophication on greenhouse gas fluxes from shallow-lake mesocosms has been shown to surpass the effects of LSWT warming alone (Bartosiewicz et al., 2019b; Davidson et al., 2015). The interaction between LSWT warming and nutrient loading highlights the complexity of greenhouse gas production mechanisms in lakes. The significance of lake warming and eutrophication control for environmental sustainability means we need models that incorporate small lakes. Here, targeted management strategies for small lakes will be particularly crucial to mitigate greenhouse gas emissions.

The extent and frequency of algal blooms has been increasing globally since 1980s, according to Landsat imagery evidence. Lakes with a smaller change in LSWT showed a decrease in bloom intensity when compared to other lakes (Dai et al., 2023; Hou et al., 2022). Based on the remote sensed global bloom dataset (Hou et al., 2022), there has been a significant increase in the bloom occurrence (BO, the ratio between the number of detected algal blooms to the number of valid satellite observations) in the last decades (Fig. 10 a). Compared with the 2000s, the global median BO increased by 44% (from 3.6% to 5.2%) in 2010s, while the global maximum bloom extent expanded by 3.14×10^4 km^2 (or 13.8%), during the same period. The bloom-stimulating effects of climate warming vary substantially under different climate zones and lacustrine environments, as well as the complex responses of LSWT to air temperatures (Elliott, 2010; Kosten et al., 2012; O'Reilly et al., 2015b). Despite restrictions on nutrient discharges in developed countries, the ongoing and widespread proliferation of algal blooms aligns closely with the recent trend of global warming (Hou et al., 2022). Lakes with smaller areas show a higher rate of increase for bloom occurrences (Fig. 10 b). This observation accords with our data on the abrupt change of LSWT warming.
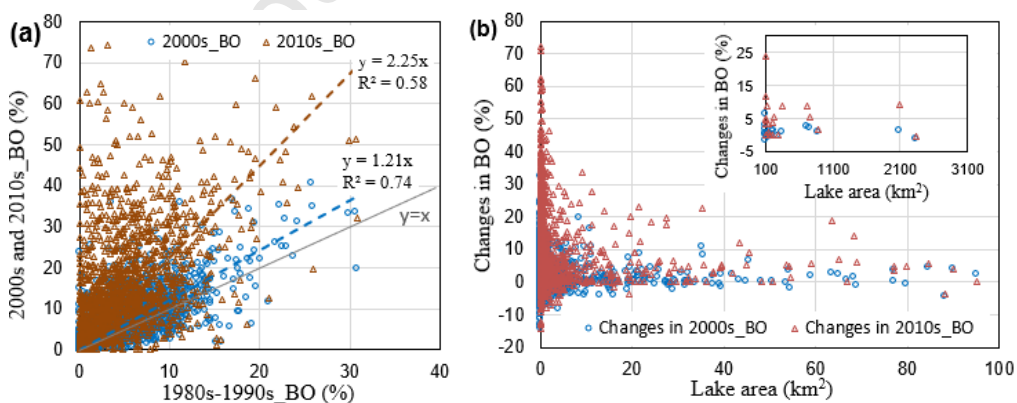

Fig. 10. The median bloom occurrence (BO) and its change in different time spans, (a) contrasting BO in 2000s and 2010s with 1980s-1990s; (b) relationship between changes in BO and lake area in 2000s and 2010s compared with that 1980s-1990s

4.4 Limitations

Due to limitations in the data accuracy of MODIS and the natural expansion or contraction of lakes, there remain uncertainties in the estimation of LSWT and its trends. Uncertainties in MODIS-derived LSWT data can arise from various factors, including atmospheric conditions, surface roughness, and sensor calibration issues. Furthermore, the revisit frequency of MODIS, which is typically 1-2 times per day, may not be sufficient to capture rapid LSWT changes, particularly during extreme weather events. These uncertainties may compromise the accuracy of the retrieved values. While MODIS data correlates well with field measurements, there is still an underestimation which warrants improvement.

The application of the HANTS method has filled the data gap and mitigates the uncertainty of LSWT (Figure 2). However, this process relies on assumptions about the periodicity and shape of frequency curves. If these assumptions do not align with actual conditions, they may introduce new uncertainties into the results. Variations in LSWT calculation methods, such as using the pixel temperature at the lake center to represent the LSWT or averaging the temperatures of all pixels covering the lake surface, can result in differences in LSWT and trend outcomes. Beyond this, given the uneven spatial distribution of lakes within the study area, uncertainties may persist in the research outcomes at the regional scale.

Our study reconstructed LSWT and analyzed trends, describing the warming or cooling mechanisms of lakes in different regions and of different types, as well as the eco-environmental response. The relationships we identify require more in-depth exploration. Despite our best efforts to include as many small lakes as possible in our research, numerous smaller water bodies, which exhibit even stronger responses to ecological environments, have not been incorporated. Because the spatial resolution of MODIS thermal products (1 km) does not yet adequately capture fine-scale variations in LSW, these water bodies were excluded. Yet, because the number of lakes larger than 0.03 km² and smaller than 1 km² globally exceeds 3 million, we know lake temperature data for the majority of small lakes are still missing from the global data set (Tong et al., 2023).

Adopting thermal infrared remote sensing imagery with higher spatial resolution will enable LSWT monitoring for more small lakes, with higher accuracy and finer temporal-spatial resolution. Integrating modelled LSWT with indictors for lake eco-environmental processes – e.g. hypoxia at lake bottoms, greenhouse gas emissions, shifts in aquatic habitat, and lake algae blooms – will further reveal the aquatic ecological and environmental effects of lake thermal changes. This research will enhance our comprehension of the potential sensitivity of lake ecosystems to climate change.

5. Conclusion

Lakes are indicators of global warming. Our study extracted LSWT from long-term MODIS imagery and used this to reconstruct LSWT data series with a combined GEE and HANTS algorithm. Our results show that, by incorporating small lakes, integration of GEE-HANTS provides a more extensive, holistic, and inclusive perspective on LSWT variations. Monitoring temperature fluctuations in lakes within a more diverse and abundant size range is a fundamental aspect of lake ecosystem research. Our LSWT research is based on lakes of various sizes across China, which are situated within diverse natural and anthropogenic environments, but it establishes a foundation for global lake studies that consider the intricate interplay of complex environmental factors. Our LSWT dataset includes small lakes to enhance the global dataset of lake water temperatures, advancing research on global lake temperature variations.

Our findings demonstrate the value of this method as follows:

1) The GEE and HANTS algorithm is efficient and accurate in detecting LSWT and LSWT trend capture even for small lakes (1-5km^2), showing good potential in LSWT analysis.

2) A general increase in LSWT at a rate of 0.24 °C per decade for 1471 lakes across China, with significant spatial and temporal variations.

3) LSWT daytime response was faster than nighttime response, but the rate of increase was higher during nighttime. EP lake zone exhibited the most significant warming trend, while some lakes in TP and NEP zones demonstrated a cooling trend driven by glacier meltwater. The majority of lakes warmed faster between 2011-2021 as compared to 2001-2010.

Our work here advances understanding of climate change impacts on lake ecosystems, revealing lake surface warming trends and spatial-temporal variations, and informs our knowledge of lake system responses to climatic factors. Our methods significantly reduce, but do not entirely eliminate, uncertainties arising from clouds and precipitation. From a methodological perspective, our innovative approach using Google Earth Engine and the Harmonic Analysis of Time Series algorithm enables accurate and efficient analysis of LSWT across vast geographical regions. These results make academic contributions to the fields of climate change and lake ecology, bridging a gap between theoretical understanding of environment change impact on small lakes and their potential practical implications for sustainable lake management and conservation efforts.

Acknowledgments

CRediT authorship contribution statement

Song Song: Writing – original draft, Funding acquisition, Conceptualization. **Jinxin Yang:** Software, Methodology. **Linjie Liu:** Data processing, Software, Visualization. **Gale Bai1:** Data processing, Investigation. **Jie Zhou:** Data curation, Methodology. **Deirdre McKay:** Writing – review & editing.

Declaration of competing interest

The authors declare that they have no known competing financial interests or personal relationships that could have appeared to influence the work reported in this paper.

Data availability

All the data used in this study are from open source.
The code can be found in the following links:
HANTS tools: https://code.earthengine.google.com/6f7c20137bd6761d5e69bef6906c986f
LSWT extraction: https://code.earthengine.google.com/24c3b8fdb353b748574c6b092bb2900d

Reference

Adrian, R., O'Reilly, C.M., Zagarese, H., Baines, S.B., Hessen, D.O., Keller, W., Livingstone, D.M., Sommaruga, R., Straile, D., Van Donk, E., Weyhenmeyer, G.A., Winder, M., 2009. Lakes as sentinels of climate change. Limnol. Oceanogr. 54, 2283–2297. https://doi.org/10.4319/lo.2009.54.6_part_2.2283

Bartosiewicz, M., Przytulska, A., Deshpande, B.N., Antoniades, D., Cortes, A., MacIntyre, S., Lehmann, M.F., Laurion, I., 2019a. Effects of climate change and episodic heat events on cyanobacteria in a eutrophic polymictic lake. Sci. Total Environ. 693, 133414. https://doi.org/10.1016/j.scitotenv.2019.07.220

Bartosiewicz, M., Przytulska, A., Lapierre, J.-F., Laurion, I., Lehmann, M.F., Maranger, R., 2019b. Hot tops, cold bottoms: Synergistic climate warming and shielding effects increase carbon burial in lakes. Limnol. Oceanogr. Lett. 4, 132–144. https://doi.org/10.1002/lol2.10117

Butcher, J.B., Nover, D., Johnson, T.E., Clark, C.M., 2015. Sensitivity of lake thermal and mixing dynamics to climate change. Clim. Change 129, 295–305. https://doi.org/10.1007/s10584-015-1326-1

Cai, H., Shimoda, Y., Mao, J., Arhonditsis, G.B., 2023. Development of a sensitivity analysis framework for aquatic biogeochemical models using machine learning. Ecol. Inform. 75, 102079. https://doi.org/10.1016/j.ecoinf.2023.102079

Dai, Y., Yang, S., Zhao, D., Hu, C., Xu, W., Anderson, D.M., Li, Y., Song, X.-P., Boyce, D.G., Gibson, L., Zheng, C., Feng, L., 2023. Coastal phytoplankton blooms expand and intensify in the 21st century. Nature 615, 280–284. https://doi.org/10.1038/s41586-023-05760-y

Davidson, T.A., Audet, J., Svenning, J.-C., Lauridsen, T.L., Søndergaard, M., Landkildehus, F., Larsen, S.E., Jeppesen, E., 2015. Eutrophication effects on greenhouse gas fluxes from shallow-lake mesocosms override those of climate warming. Glob. Change Biol. 21, 4449–4463. https://doi.org/10.1111/gcb.13062

Descy, J.-P., Leprieur, F., Pirlot, S., Leporcq, B., Van Wichelen, J., Peretyatko, A., Teissier, S., Codd, G.A., Triest, L., Vyverman, W., Wilmotte, A., 2016. Identifying the factors determining blooms of cyanobacteria in a set of shallow lakes. Ecol. Inform. 34, 129–138. https://doi.org/10.1016/j.ecoinf.2016.05.003

Elliott, J.A., 2010. The seasonal sensitivity of Cyanobacteria and other phytoplankton to changes in flushing rate and water temperature. Glob. Change Biol. 16, 864–876. https://doi.org/10.1111/j.1365-2486.2009.01998.x

Fairall, C.W., Bradley, E.F., Godfrey, J.S., Wick, G.A., Edson, J.B., Young, G.S., 1996. Cool-skin and warm-layer effects on sea surface temperature. J. Geophys. Res. Oceans 101, 1295–1308. https://doi.org/10.1029/95JC03190

Feng, L., Pi, X., Luo, Q., Li, W., 2023. Reconstruction of long-term high-resolution lake variability: Algorithm improvement and applications in China. Remote Sens. Environ. 297, 113775. https://doi.org/10.1016/j.rse.2023.113775

Filiz, N., Işkın, U., Beklioğlu, M., Öğlü, B., Cao, Y., Davidson, T.A., Søndergaard, M., Lauridsen, T.L., Jeppesen, E., 2020. Phytoplankton Community Response to Nutrients, Temperatures, and a Heat Wave in Shallow Lakes: An Experimental Approach. Water 12, 3394. https://doi.org/10.3390/w12123394

Gorelick, N., Hancher, M., Dixon, M., Ilyushchenko, S., Thau, D., Moore, R., 2017. Google Earth

Engine: Planetary-scale geospatial analysis for everyone. Remote Sens. Environ., Big Remotely Sensed Data: tools, applications and experiences 202, 18–27. https://doi.org/10.1016/j.rse.2017.06.031

Guo, L., Zheng, H., Wu, Y., Fan, L., Wen, M., Li, J., Zhang, F., Zhu, L., Zhang, B., 2022. An integrated dataset of daily lake surface water temperature over the Tibetan Plateau. Earth Syst. Sci. Data 14, 3411–3422. https://doi.org/10.5194/essd-14-3411-2022

Hanson, P.C., Carpenter, S.R., Cardille, J.A., Coe, M.T., Winslow, L.A., 2007. Small lakes dominate a random sample of regional lake characteristics. Freshw. Biol. 52, 814–822. https://doi.org/10.1111/j.1365-2427.2007.01730.x

Ho, J.C., Michalak, A.M., Pahlevan, N., 2019. Widespread global increase in intense lake phytoplankton blooms since the 1980s. Nature 574, 667–670. https://doi.org/10.1038/s41586-019-1648-7

Holgerson, M.A., Raymond, P.A., 2016. Large contribution to inland water CO2 and CH4 emissions from very small ponds. Nat. Geosci. 9, 222–226. https://doi.org/10.1038/ngeo2654

Hou, X., Feng, L., Dai, Y., Hu, C., Gibson, L., Tang, J., Lee, Z., Wang, Y., Cai, X., Liu, J., Zheng, Y., Zheng, C., 2022. Global mapping reveals increase in lacustrine algal blooms over the past decade. Nat. Geosci. 15, 130–134. https://doi.org/10.1038/s41561-021-00887-x

Hu, M., Ma, R., Xue, K., Cao, Z., Xiong, J., Loiselle, S.A., Shen, M., Hou, X., 2024. Eutrophication evolution of lakes in China: Four decades of observations from space. J. Hazard. Mater. 470, 134225. https://doi.org/10.1016/j.jhazmat.2024.134225

Huang, L., Wang, J., Zhu, L., Ju, J., Daut, G., 2017. The Warming of Large Lakes on the Tibetan Plateau: Evidence From a Lake Model Simulation of Nam Co, China, During 1979–2012. J. Geophys. Res. Atmospheres 122, 13,095-13,107. https://doi.org/10.1002/2017JD027379

Huang, L., Wang, X., Sang, Y., Tang, S., Jin, L., Yang, H., Ottlé, C., Bernus, A., Wang, S., Wang, C., Zhang, Y., 2021. Optimizing Lake Surface Water Temperature Simulations Over Large Lakes in China With FLake Model. Earth Space Sci. 8, e2021EA001737. https://doi.org/10.1029/2021EA001737

Huang, L., Wang, X., Yan, Y., Jin, L., Yang, K., Chen, A., Zheng, R., Ottlé, C., Wang, C., Cui, Y., Piao, S., 2023. Attribution of Lake Surface Water Temperature Change in Large Lakes Across China Over Past Four Decades. J. Geophys. Res. Atmospheres 128, e2022JD038465. https://doi.org/10.1029/2022JD038465

Jia, J., Dungait, J.A.J., Yu, G., Cui, T., Gao, Y., 2024. Nutrient enrichment and climate warming drive carbon production of global lake ecosystems. Earth-Sci. Rev. 258, 104968. https://doi.org/10.1016/j.earscirev.2024.104968

Jia, T., Yang, K., Peng, Z., Tang, L., Duan, H., Luo, Y., 2022. Review on the Change Trend, Attribution Analysis, Retrieval, Simulation, and Prediction of Lake Surface Water Temperature. IEEE J. Sel. Top. Appl. Earth Obs. Remote Sens. 15, 6324–6355. https://doi.org/10.1109/JSTARS.2022.3188788

Jiang, L., Nielsen, K., Andersen, O.B., Bauer-Gottwein, P., 2017. Monitoring recent lake level variations on the Tibetan Plateau using CryoSat-2 SARIn mode data. J. Hydrol. 544, 109–124. https://doi.org/10.1016/j.jhydrol.2016.11.024

Kosten, S., Huszar, V.L.M., Bécares, E., Costa, L.S., van Donk, E., Hansson, L.-A., Jeppesen, E., Kruk, C., Lacerot, G., Mazzeo, N., De Meester, L., Moss, B., Lürling, M., Nõges, T., Romo, S., Scheffer, M., 2012. Warmer climates boost cyanobacterial dominance in shallow lakes. Glob. Change

Biol. 18, 118–126. https://doi.org/10.1111/j.1365-2486.2011.02488.x

Kumar, A., Mishra, S., Bakshi, S., Upadhyay, P., Thakur, T.K., 2023. Response of eutrophication and water quality drivers on greenhouse gas emissions in lakes of China: A critical analysis. Ecohydrology 16, e2483. https://doi.org/10.1002/eco.2483

Li, X., Peng, S., Xi, Y., Woolway, R.I., Liu, G., 2022. Earlier ice loss accelerates lake warming in the Northern Hemisphere. Nat. Commun. 13, 5156. https://doi.org/10.1038/s41467-022-32830-y

Liu, G., Ou, W., Zhang, Y., Wu, T., Zhu, G., Shi, K., Qin, B., 2015. Validating and Mapping Surface Water Temperatures in Lake Taihu: Results From MODIS Land Surface Temperature Products. IEEE J. Sel. Top. Appl. Earth Obs. Remote Sens. 8, 1230–1244. https://doi.org/10.1109/JSTARS.2014.2386333

Lürling, M., Mucci, M., 2020. Mitigating eutrophication nuisance: in-lake measures are becoming inevitable in eutrophic waters in the Netherlands. Hydrobiologia 847, 4447–4467. https://doi.org/10.1007/s10750-020-04297-9

Meerhoff, M., Audet, J., Davidson, T.A., De Meester, L., Hilt, S., Kosten, S., Liu, Z., Mazzeo, N., Paerl, H., Scheffer, M., Jeppesen, E., 2022. Feedback between climate change and eutrophication: revisiting the allied attack concept and how to strike back. Inland Waters 12, 187–204. https://doi.org/10.1080/20442041.2022.2029317

Menenti, M., Azzali, S., Verhoef, W., van Swol, R., 1993. Mapping agroecological zones and time lag in vegetation growth by means of fourier analysis of time series of NDVI images. Adv. Space Res. 13, 233–237. https://doi.org/10.1016/0273-1177(93)90550-U

Menenti, M., Malamiri, H.R.G., Shang, H., Alfieri, S.M., Maffei, C., Jia, L., 2016. Observing the Response of Terrestrial Vegetation to Climate Variability Across a Range of Time Scales by Time Series Analysis of Land Surface Temperature, in: Multitemporal Remote Sensing. Springer, Cham, pp. 277–315. https://doi.org/10.1007/978-3-319-47037-5_14

Meng, H., Zhang, J., Zheng, Z., Song, Y., Lai, Y., 2024. Classification of inland lake water quality levels based on Sentinel-2 images using convolutional neural networks and spatiotemporal variation and driving factors of algal bloom. Ecol. Inform. 80, 102549. https://doi.org/10.1016/j.ecoinf.2024.102549

Noori, R., Woolway, R.I., Jun, C., Bateni, S.M., Naderian, D., Partani, S., Maghrebi, M., Pulkkanen, M., 2023. Multi-decadal change in summer mean water temperature in Lake Konnevesi, Finland (1984–2021). Ecol. Inform. 78, 102331. https://doi.org/10.1016/j.ecoinf.2023.102331

Oki, T., Kanae, S., 2006. Global hydrological cycles and world water resources. Science 313, 1068–1072. https://doi.org/10.1126/science.1128845

O'Reilly, C.M., Sharma, S., Gray, D.K., Hampton, S.E., Read, J.S., Rowley, R.J., Schneider, P., Lenters, J.D., McIntyre, P.B., Kraemer, B.M., Weyhenmeyer, G.A., Straile, D., Dong, B., Adrian, R., Allan, M.G., Anneville, O., Arvola, L., Austin, J., Bailey, J.L., Baron, J.S., Brookes, J.D., de Eyto, E., Dokulil, M.T., Hamilton, D.P., Havens, K., Hetherington, A.L., Higgins, S.N., Hook, S., Izmest'eva, L.R., Joehnk, K.D., Kangur, K., Kasprzak, P., Kumagai, M., Kuusisto, E., Leshkevich, G., Livingstone, D.M., MacIntyre, S., May, L., Melack, J.M., Mueller-Navarra, D.C., Naumenko, M., Noges, P., Noges, T., North, R.P., Plisnier, P.-D., Rigosi, A., Rimmer, A., Rogora, M., Rudstam, L.G., Rusak, J.A., Salmaso, N., Samal, N.R., Schindler, D.E., Schladow, S.G., Schmid, M., Schmidt, S.R., Silow, E., Soylu, M.E., Teubner, K., Verburg, P., Voutilainen, A., Watkinson, A., Williamson, C.E., Zhang, G., 2015a. Rapid and highly variable warming of

lake surface waters around the globe. Geophys. Res. Lett. 42, 10,773-10,781. https://doi.org/10.1002/2015GL066235

O'Reilly, C.M., Sharma, S., Gray, D.K., Hampton, S.E., Read, J.S., Rowley, R.J., Schneider, P., Lenters, J.D., McIntyre, P.B., Kraemer, B.M., Weyhenmeyer, G.A., Straile, D., Dong, B., Adrian, R., Allan, M.G., Anneville, O., Arvola, L., Austin, J., Bailey, J.L., Baron, J.S., Brookes, J.D., de Eyto, E., Dokulil, M.T., Hamilton, D.P., Havens, K., Hetherington, A.L., Higgins, S.N., Hook, S., Izmest'eva, L.R., Joehnk, K.D., Kangur, K., Kasprzak, P., Kumagai, M., Kuusisto, E., Leshkevich, G., Livingstone, D.M., MacIntyre, S., May, L., Melack, J.M., Mueller-Navarra, D.C., Naumenko, M., Noges, P., Noges, T., North, R.P., Plisnier, P.-D., Rigosi, A., Rimmer, A., Rogora, M., Rudstam, L.G., Rusak, J.A., Salmaso, N., Samal, N.R., Schindler, D.E., Schladow, S.G., Schmid, M., Schmidt, S.R., Silow, E., Soylu, M.E., Teubner, K., Verburg, P., Voutilainen, A., Watkinson, A., Williamson, C.E., Zhang, G., 2015b. Rapid and highly variable warming of lake surface waters around the globe. Geophys. Res. Lett. 42, 10,773-10,781. https://doi.org/10.1002/2015GL066235

O'Sullivan, A.M., Devito, K.J., Curry, R.A., 2019. The influence of landscape characteristics on the spatial variability of river temperatures. CATENA 177, 70–83. https://doi.org/10.1016/j.catena.2019.02.006

Peng, Z., Yang, J., Luo, Y., Yang, K., Shang, C., 2021. Impact of climate warming on the surface water temperature of plateau lake. Acta Geophys. 69, 895–907. https://doi.org/10.1007/s11600-021-00581-x

Pi, X., Luo, Q., Feng, L., Xu, Y., Tang, J., Liang, X., Ma, E., Cheng, R., Fensholt, R., Brandt, M., Cai, X., Gibson, L., Liu, J., Zheng, C., Li, W., Bryan, B.A., 2022. Mapping global lake dynamics reveals the emerging roles of small lakes. Nat. Commun. 13, 5777. https://doi.org/10.1038/s41467-022-33239-3

Piccolroaz, S., Woolway, R.I., Merchant, C.J., 2020a. Global reconstruction of twentieth century lake surface water temperature reveals different warming trends depending on the climatic zone. Clim. Change 160, 427–442. https://doi.org/10.1007/s10584-020-02663-z

Piccolroaz, S., Woolway, R.I., Merchant, C.J., 2020b. Global reconstruction of twentieth century lake surface water temperature reveals different warming trends depending on the climatic zone. Clim. Change 160, 427–442. https://doi.org/10.1007/s10584-020-02663-z

Piccolroaz, S., Zhu, S., Ladwig, R., Carrea, L., Oliver, S., Piotrowski, A.P., Ptak, M., Shinohara, R., Sojka, M., Woolway, R.I., Zhu, D.Z., 2024. Lake Water Temperature Modeling in an Era of Climate Change: Data Sources, Models, and Future Prospects. Rev. Geophys. 62, e2023RG000816. https://doi.org/10.1029/2023RG000816

Rao, K., Cao, X., Wang, Y., Zhang, Y., Huang, H., Ma, Y., Xu, J., 2024. Spatial-temporal distributions of phytoplankton shifting, chlorophyll-a, and their influencing factors in shallow lakes using remote sensing. Ecol. Inform. 82, 102765. https://doi.org/10.1016/j.ecoinf.2024.102765

Ratajczak, Z., Carpenter, S.R., Ives, A.R., Kucharik, C.J., Ramiadantsoa, T., Stegner, M.A., Williams, J.W., Zhang, J., Turner, M.G., 2018. Abrupt Change in Ecological Systems: Inference and Diagnosis. Trends Ecol. Evol. 33, 513–526. https://doi.org/10.1016/j.tree.2018.04.013

Sharaf, N., Fadel, A., Bresciani, M., Giardino, C., B Vinçon-Leite, 2019. Lake surface temperature retrieval from Landsat-8 and retrospective analysis in Karaoun Reservoir, Lebanon. J. Appl. Remote Sens. 13, 1-. https://doi.org/10.1117/1.JRS.13.044505

Shi, K., Wang, W., 2023. Daily scale dataset of lake surface water temperature and lake surface water

temperature after removing heat extremes in China (1985-2022). https://doi.org/10.11888/Terre.tpdc.300801. https://cstr.cn/18406.11.Terre.tpdc.300801.

Shi, K., Wang, X., 2022. Dataset of lake surface water temperature in China (1950-2100). https://doi.org/10.11888/Terre.tpdc.300662. https://cstr.cn/18406.11.Terre.tpdc.300662.

Song, K., Wang, Min, Du, J., Yuan, Y., Ma, J., Wang, Ming, Mu, G., 2016. Spatiotemporal Variations of Lake Surface Temperature across the Tibetan Plateau Using MODIS LST Product. Remote Sens. 8, 854. https://doi.org/10.3390/rs8100854

Song, S., Cao, Z., Wu, Z., Chuai, X., 2022. Spatial and Temporal Dynamics of Surface Water in China from the 1980s to 2015 Based on Remote Sensing Monitoring. Chin. Geogr. Sci. 32, 174–188. https://doi.org/10.1007/s11769-021-1252-2

Tamiminia, H., Salehi, B., Mahdianpari, M., Quackenbush, L., Adeli, S., Brisco, B., 2020. Google Earth Engine for geo-big data applications: A meta-analysis and systematic review. ISPRS J. Photogramm. Remote Sens. 164, 152–170. https://doi.org/10.1016/j.isprsjprs.2020.04.001

Tavares, M.H., Cunha, A.H.F., Motta-Marques, D., Ruhoff, A.L., Cavalcanti, J.R., Fragoso, C.R., Martín Bravo, J., Munar, A.M., Fan, F.M., Rodrigues, L.H.R., 2019. Comparison of Methods to Estimate Lake-Surface-Water Temperature Using Landsat 7 ETM+ and MODIS Imagery: Case Study of a Large Shallow Subtropical Lake in Southern Brazil. Water 11, 168. https://doi.org/10.3390/w11010168

Tavares, M.H., Cunha, A.H.F., Motta-Marques, D., Ruhoff, A.L., Fragoso, C.R., Munar, A.M., Bonnet, M.-P., 2020. Derivation of consistent, continuous daily river temperature data series by combining remote sensing and water temperature models. Remote Sens. Environ. 241, 111721. https://doi.org/10.1016/j.rse.2020.111721

Tong, Y., Feng, L., Wang, X., Pi, X., Xu, W., Woolway, R.I., 2023. Global lakes are warming slower than surface air temperature due to accelerated evaporation. Nat. Water 1, 929–940. https://doi.org/10.1038/s44221-023-00148-8

VERHOEF, W., MENENTI, M., AZZALI, S., 1996. Cover A colour composite of NOAA-AVHRR-NDVI based on time series analysis (1981-1992). Int. J. Remote Sens. https://doi.org/10.1080/01431169608949001

Verpoorter, C., Kutser, T., Seekell, D.A., Tranvik, L.J., 2014. A global inventory of lakes based on high-resolution satellite imagery. Geophys. Res. Lett. 41, 6396–6402. https://doi.org/10.1002/2014GL060641

Virdis, S.G.P., Kongwarakom, S., Juneng, L., Padedda, B.M., Shrestha, S., 2024. Historical and projected response of Southeast Asian lakes surface water temperature to warming climate. Environ. Res. 247, 118412. https://doi.org/10.1016/j.envres.2024.118412

Virdis, S.G.P., Soodcharoen, N., Lugliè, A., Padedda, B.M., 2020. Estimation of satellite-derived lake water surface temperatures in the western Mediterranean: Integrating multi-source, multi-resolution imagery and a long-term field dataset using a time series approach. Sci. Total Environ. 707, 135567. https://doi.org/10.1016/j.scitotenv.2019.135567

Wan, W., Li, H., Xie, H., Hong, Y., Long, D., Zhao, L., Han, Z., Cui, Y., Liu, B., Wang, C., Yang, W., 2017. A comprehensive data set of lake surface water temperature over the Tibetan Plateau derived from MODIS LST products 2001–2015. Sci. Data 4, 170095. https://doi.org/10.1038/sdata.2017.95

Wan, W., Zhao, L., Xie, H., Liu, B., Li, H., Cui, Y., Ma, Y., Hong, Y., 2018. Lake Surface Water Temperature Change Over the Tibetan Plateau From 2001 to 2015: A Sensitive Indicator of the Warming

Climate. Geophys. Res. Lett. 45, 11,177-11,186. https://doi.org/10.1029/2018GL078601

Wan, Z., 2008. New refinements and validation of the MODIS Land-Surface Temperature/Emissivity products. Remote Sens. Environ. 112, 59–74. https://doi.org/10.1016/j.rse.2006.06.026

Wang, W., Shi, K., Wang, X., Zhang, Yunlin, Qin, B., Zhang, Yibo, Woolway, R.I., 2024. The impact of extreme heat on lake warming in China. Nat. Commun. 15, 70. https://doi.org/10.1038/s41467-023-44404-7

Wang, X., Shi, K., Zhang, Yunlin, Qin, B., Zhang, Yibo, Wang, W., Woolway, R.I., Piao, S., Jeppesen, E., 2023. Climate change drives rapid warming and increasing heatwaves of lakes. Sci. Bull. 68, 1574–1584. https://doi.org/10.1016/j.scib.2023.06.028

Winslow, L.A., Leach, T.H., Rose, K.C., 2018. Global lake response to the recent warming hiatus. Environ. Res. Lett. 13, 054005. https://doi.org/10.1088/1748-9326/aab9d7

Woelmer, W.M., Thomas, R.Q., Olsson, F., Steele, B.G., Weathers, K.C., Carey, C.C., 2024. Process-based forecasts of lake water temperature and dissolved oxygen outperform null models, with variability over time and depth. Ecol. Inform. 83, 102825. https://doi.org/10.1016/j.ecoinf.2024.102825

Woolway, R.I., Kraemer, B.M., Lenters, J.D., Merchant, C.J., O'Reilly, C.M., Sharma, S., 2020. Global lake responses to climate change. Nat. Rev. Earth Environ. 1, 388–403. https://doi.org/10.1038/s43017-020-0067-5

Woolway, R.I., Merchant, C.J., 2019. Worldwide alteration of lake mixing regimes in response to climate change. Nat. Geosci. 12, 271–276. https://doi.org/10.1038/s41561-019-0322-x

Wu, Y., Huang, A., Li, X., Wen, L., Lazhu, Li, J., 2024. Thermal Response of Large Seasonally Ice-Covered Lakes Over Tibetan Plateau to Climate Change. J. Geophys. Res. Atmosheres 129, e2023JD039935. https://doi.org/10.1029/2023JD039935

Xiao, Q., Duan, H., Qin, B., Hu, Z., Zhang, M., Qi, T., Lee, X., 2022. Eutrophication and temperature drive large variability in carbon dioxide from China's Lake Taihu. Limnol. Oceanogr. 67, 379–391. https://doi.org/10.1002/lno.11998

Xie, C., Zhang, X., Zhuang, L., Zhu, R., Guo, J., 2022. Analysis of surface temperature variation of lakes in China using MODIS land surface temperature data. Sci. Rep. 12, 2415. https://doi.org/10.1038/s41598-022-06363-9

Xie, F., Fan, H., 2021. Deriving drought indices from MODIS vegetation indices (NDVI/EVI) and Land Surface Temperature (LST): Is data reconstruction necessary? Int. J. Appl. Earth Obs. Geoinformation 101, 102352. https://doi.org/10.1016/j.jag.2021.102352

Xu, Y., Shen, Y., Wu, Z., 2013. Spatial and Temporal Variations of Land Surface Temperature Over the Tibetan Plateau Based on Harmonic Analysis. Mt. Res. Dev. 33, 85–94. https://doi.org/10.1659/MRD-JOURNAL-D-12-00090.1

Yaghouti, M., Heidarzadeh, N., Ulloa, H.N., Nakhaei, N., 2023. The impacts of climate change on thermal stratification and dissolved oxygen in the temperate, dimictic Mississippi Lake, Ontario. Ecol. Inform. 75, 102087. https://doi.org/10.1016/j.ecoinf.2023.102087

Yang, K., Yu, Z., Luo, Y., Zhou, X., Shang, C., 2019. Spatial-Temporal Variation of Lake Surface Water Temperature and Its Driving Factors in Yunnan-Guizhou Plateau. Water Resour. Res. 55, 4688–4703. https://doi.org/10.1029/2019WR025316

Zhang, G., Yao, T., Chen, W., Zheng, G., Shum, C.K., Yang, K., Piao, S., Sheng, Y., Yi, S., Li, J., O'Reilly, C.M., Qi, S., Shen, S.S.P., Zhang, H., Jia, Y., 2019. Regional differences of lake evolution across China during 1960s–2015 and its natural and anthropogenic causes. Remote Sens. Environ.

221, 386–404. https://doi.org/10.1016/j.rse.2018.11.038

Zhang, G., Yao, T., Xie, H., Qin, J., Ye, Q., Dai, Y., Guo, R., 2014. Estimating surface temperature changes of lakes in the Tibetan Plateau using MODIS LST data. J. Geophys. Res. Atmospheres 119, 8552–8567. https://doi.org/10.1002/2014JD021615

Zhou, J., Jia, L., Menenti, M., 2015. Reconstruction of global MODIS NDVI time series: Performance of Harmonic ANalysis of Time Series (HANTS). Remote Sens. Environ. 163, 217–228. https://doi.org/10.1016/j.rse.2015.03.018

Zhou, J., Jia, L., Menenti, M., Liu, X., 2021. Optimal Estimate of Global Biome—Specific Parameter Settings to Reconstruct NDVI Time Series with the Harmonic ANalysis of Time Series (HANTS) Method. Remote Sens. 13, 4251. https://doi.org/10.3390/rs13214251

Zhou, J., Menenti, M., Jia, L., Gao, B., Zhao, F., Cui, Y., Xiong, X., Liu, X., Li, D., 2023. A scalable software package for time series reconstruction of remote sensing datasets on the Google Earth Engine platform. Int. J. Digit. Earth 16, 988–1007. https://doi.org/10.1080/17538947.2023.2192004

Zhu, L., 2021. In-situ water quality parameters of the lakes on the Tibetan Plateau (2009-2020). Natl. Tibet. Plateau Data Cent. https://doi.org/10.11888/Geogra.tpdc.271450

Highlights

1. GEE-HANTS enables efficient and accurate LSWT detection, even in small lakes.
2. LSWT increased at 0.24°C/decade with spatial/temporal variations.
3. For 2001-2010, the nighttime rate of increase LSWT was greater than the daytime rate of increase.
4. Daytime LSWT changed abruptly in 2010, before a shift in nighttime LSWT